Latitude survey observations of neutron monitor multiplicity

J. W. Bieber,[1] J. M. Clem,[1] M. L. Duldig,[2] P. A. Evenson,[1] J. E. Humble,[3] and R. Pyle[1]

Received 23 March 2004; revised 22 June 2004; accepted 22 October 2004; published 17 December 2004.

[1] We have recently augmented the electronics for our neutron monitor (NM) latitude survey so as to record the elapsed time (δT) between detected neutrons in each proportional tube, in order to examine time correlations in the data as a function of cutoff rigidity and primary spectrum. We quantify the dependence of counting rate on dead time, with particular focus on the longer dead times that were once employed in FSU/Russian stations. Our observations show that monitor dead time has little influence on the observed depth of Forbush decreases, indicating that the cosmic ray spectral shape is little changed in the decrease. However, the use of a different dead time significantly alters the response of the monitor as a function of cutoff rigidity. In spite of the general success of our calculation in reproducing the data, unexplained discrepancies are still present. *INDEX TERMS:* 2104 Interplanetary Physics: Cosmic rays; 2479 Ionosphere: Solar radiation and cosmic ray effects; 3005 Marine Geology and Geophysics: Geomagnetism (1550); 7807 Space Plasma Physics: Charged particle motion and acceleration; 0350 Atmospheric Composition and Structure: Pressure, density, and temperature; *KEYWORDS:* neutron monitor, geomagnetic field, cosmic rays

Citation: Bieber, J. W., J. M. Clem, M. L. Duldig, P. A. Evenson, J. E. Humble, and R. Pyle (2004), Latitude survey observations of neutron monitor multiplicity, *J. Geophys. Res.*, *109*, A12106, doi:10.1029/2004JA010493.

1. Introduction

[2] Characterization of the ground-based neutron monitor as a primary cosmic ray detector requires understanding the relationship between the observed count rate and the energy dependent flux of cosmic rays at the top of the atmosphere. This relationship, typically known as the yield function, is the combined result of particle transport through the atmosphere and detection efficiency of a neutron monitor. Those primary cosmic rays with rigidity above the local geomagnetic cutoff enter the atmosphere and undergo multiple interactions producing secondary particles which may reach ground level. In a neutron monitor, BF_3 or ^{3}He filled proportional counters detect neutrons produced locally by the secondary particles interacting in a lead (Pb) target, termed the producer. Time correlations among the detected neutrons or counts in the monitor contain information about the incident energy of the secondary, which in turn retains some memory of the energy of the primary. Generally, the term multiplicity is used to refer to time correlations among individual detector counts. More specifically, considering a specific time window, an event of multiplicity N refers to the occurrence of N counts within the window.

[3] A neutron monitor latitude survey is conducted with a mobile neutron monitor that records counting rates during passage through a range of geomagnetic cutoffs [*Moraal et al.*, 1989; *Nagashima et al.*, 1989; *Villoresi et al.*, 2000; *Iucci et al.*, 2000; *Dorman et al.*, 2000; *Bieber et al.*, 2003]. The scientific motivation behind such a survey is threefold: to improve knowledge of geomagnetic cutoffs, to study the primary cosmic ray spectrum, and to understand the neutron monitor energy response function. Equation (1) provides a mathematical description of the relationship between parameters relevant to a latitude survey in the usual approximation:

$$N(P_C) = \int_{P_C}^{\infty} S(P) j(P) dP. \quad (1)$$

$N(P_C)$ is the neutron monitor counting rate, P_C is the geomagnetic cutoff, $S(P)$ is the neutron monitor yield function, and $j(P)$ is the primary cosmic ray spectrum expressed as a function of rigidity P. This spectrum is influenced by magnetic fields in interplanetary space and thus varies with solar activity.

[4] The earliest known measurement of the latitude dependence of multiplicity was performed by *Dyring and Sporre* [1966] using a two-tube IGY monitor. Subsequently, other surveys have been conducted, such as that of *Aleksanyan et al.* [1979]. In these surveys the multiplicity of an event was determined by opening a time gate initiated by a single count and adding the additional counts that occur during the gate length. The total number of counts in each event determines the multiplicity level. Each level has

[1]Bartol Research Institute, University of Delaware, Newark, Delaware, USA.
[2]Australian Antarctic Division, Kingston, Tasmania, Australia.
[3]School of Mathematics and Physics, University of Tasmania, Hobart, Tasmania, Australia.

0148-0227/04/2004JA010493$09.00

an associated response function corresponding to a different median rigidity of primary particles but, owing to the complicated nature of the neutron monitor detection process and the broad energy variations of the ground-level secondaries for the same initial primary energy, extracting the primary spectrum from a multiplicity distribution is very difficult.

[5] To gain a better understanding of this process and to provide additional checks of our simulations, we have augmented the electronics in our three-tube NM-64 latitude survey station to measure the elapsed time (δT) between counts from each proportional tube. *Hatton and Tomlinson* [1968] made similar measurements with IGY and NM64 monitors at one location, but to our knowledge this is the first application of this technique to a latitude survey, so as to preserve full information on the time structure of the data and allow construction of data sets that simulate exactly the performance of monitors using other approaches.

[6] We present an initial analysis of data acquired during the northbound segment of the 2000–2001 Bartol/Tasmania latitude survey [*Clem et al.*, 1997; *Bieber et al.*, 2003] and compare these data to a numerical simulation. As an initial application of our results, we quantify and discuss the response differences between our stations and the Russian/FSU stations operating prior to the mid-1980s. These stations by design had a much longer dead time than the standard NM64 [*Blokh et al.*, 1971]. With the exception of the Apatity station, currently all Russian/FSU stations report counts using nearly the same dead time as our stations, while Apatity reports two count rates, one using the short dead time similar to our stations and the other using the original Russian/FSU long dead time (E. Eroshenko, private communication, 2004).

2. Neutron Monitor Multiplicity

[7] Multiple counts in a neutron monitor occurring within a period of a few milliseconds can be produced by multiparticle showers containing a hadron density of roughly >2 m^{-2}. With an interaction length of $\sim$90 g/cm^2, a secondary hadron observed at sea level is more than 10 inelastic interactions removed from the parent primary [*Particle Data Group*, 2002]. Typically, the last atmospheric interaction occurred 1/2 interaction length (350 m at sea level) above the monitor; thus the detection of multiple incident particles requires that the angular separation between the resulting secondaries produced in the interaction must be less than 3×10^{-3} radians (not considering scattering effects). This effect was included in some of the simulations, and we determined that it changes the δT distribution by less than 1% at any point and the overall normalization by less than 0.1%. Because such inclusion greatly increases the running time of the simulation, we ignore this process in the remainder of the discussion.

[8] The dominant source of multiplicity is generation of multiple neutrons in the producer by a single incident secondary cosmic ray. Roughly 60% of the energetic hadrons that enter the producer of a neutron monitor produce an inelastic interaction. The n-Pb interaction process can generally be separated into two stages. During the first stage, knock-on nucleons, heavy fragments, and mesons are generated with a wide range of energies and a scattering distribution strongly biased in the direction of the incident particle's momentum. Owing to their high energy, these secondary particles typically escape detection. The next stage of the process is the deexcitation phase in which additional particles are emitted from the wounded target nucleus. Most of these emissions are evaporated neutrons that are characterized by a spectrum peaked near 1.0 MeV (mean of 2.5 MeV) and an isotropic angular distribution. The average number of evaporated neutrons generated in an interaction is energy dependent and can be roughly described as a power law

$$\nu_n = 25E^{0.4}, \tag{2}$$

where ν_n is the average number of evaporated neutrons and E is the energy (GeV) of the incident particle [*Hughes et al.*, 1964; *Shen*, 1968; *Hatton*, 1971]. Therefore a Pb interaction involving a 100 MeV incident neutron produces an average of 10 evaporation neutrons.

[9] The probability of detecting an evaporation neutron produced from a Pb interaction in a monitor depends on its initial energy and location. *Hatton* [1971] considered this problem analytically and estimated the average efficiency of detecting an evaporation neutron through integrating the expected neutron production from Pb interactions uniformly distributed over a NM-64 producer volume. The resulting calculation yielded detection efficiencies ranging from 2% for a 20 MeV evaporation neutron to 10% at 0.2 MeV with 6.5% at 2.5 MeV (the mean evaporation neutron energy for a Pb interaction). Using these results and assuming all evaporation energies are 2.5 MeV, the probability of detecting one or more evaporation neutrons can be easily calculated utilizing the binomial distribution. As an example, a Pb interaction with a 100 MeV incident neutron should yield roughly 10 evaporation neutrons ($\nu_n = 25\ E^{0.4} \approx 10$ for E = 0.1 GeV); therefore the efficiency of detecting evaporation neutrons from a 100 MeV incident neutron interaction is determined to be roughly 49% for 1 or more, 13% for 2 or more, 2% for 3 or more, and so forth, resulting in a specific multiplicity distribution for this incident energy. Multiple detections of evaporation neutrons from the same interaction do not occur instantaneously but exhibit a characteristic time distribution defined by location of the interaction and the diffusion properties and geometry of the materials used in a neutron monitor.

3. Method

[10] Each detector count is recorded by custom electronics and the elapsed time between counts is derived from a 16 bit scaler internal to a microcontroller. This scaler advances uniformly at a frequency derived from an external oscillator (3.6864 MHz divided by 8), thus each tick of the clock is 2.17 μs.

[11] When the appropriate logic in the microcontroller is armed, the detector counting discriminator latches the internal scaler in a register and generates an interrupt to the microcontroller. Processing this interrupt takes approximately 95 μs to the point where the circuit may be rearmed. This determines the minimum time separation that can be measured. Keeping track of scaler overflows would increase this latency dramatically, so we simply allow the scaler to

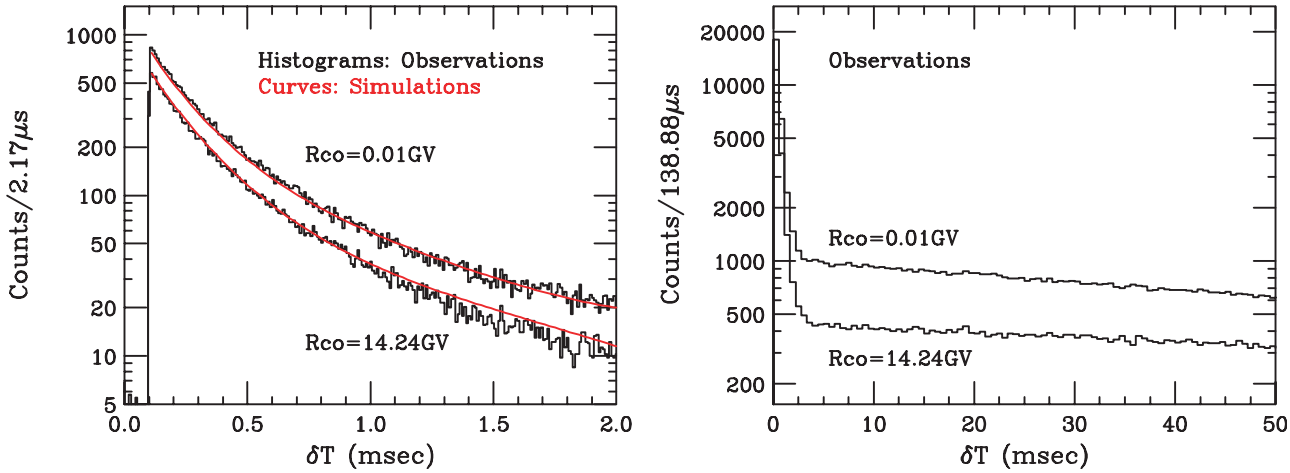

Figure 1. (left) Distribution of the elapsed time δT (modulo 142 ms) between measured single tube counts for 14.2 GV cutoff rigidity (lower curve and data) and 0.01 GV cutoff rigidity (upper curve and data). The histograms represent the observed data. The curves represent simulated data scaled by a factor of 0.7. (right) The same data on a compressed scale illustrating the transition from correlated to uncorrelated counts.

cycle with the result that times are recorded modulo approximately 142 ms ($\approx 2^{16} \times 2.17$ μs), which is the full cycle time of our 16 bit clock scaler.

[12] Primary readout of the detector electronics takes place once per second. A count of the total number of discriminator firings (from a hardware scaler) is transmitted, together with various housekeeping information. Part of this housekeeping information is the timing scaler reading and pulse height for the first 12 sequential discriminator firings.

[13] For the present analysis, we ignore the first scaler reading (since the actual latency of that is unknown due to the time occupied by the readout cycle) and compute the delay times first-to-second, second-to-third, and so forth. Histograms of these times (1024 channels) are accumulated and recorded for each hour.

[14] Figure 1 displays the δT distribution of a single tube for two different geographic locations on the 2000–2001 Bartol-Tasmania latitude survey. The truncation at the low end (95 μs) of the distribution is the result of the dead time in the multiplicity circuit. It should be noted that the corresponding dead time in the counting circuit is 20 μs, the NM64 standard value. The effective vertical rigidity cutoffs of these two locations were 14.24 GV (lower curve and data) and 0.01 GV (upper curve and data) and the elapsed exposure time at each location is 24 hours. These particular locations were chosen such that the count rate of the polar neutron monitor (McMurdo) was similar for these periods of the survey.

[15] Data in the left panel are compared to simulations. The simulation reproduces the shape of the distribution well, but the amplitude differs by an overall, uniform scaling factor of 0.7. This is either the result of unknown detection efficiencies in the neutron counters or inaccuracies in the model. Recent accelerator calibration of neutron monitors compared to our simulation show normalization differences from 10% to 20% [*Clem*, 1999; *Shibata et al.*, 1999; *Birattari et al.*, 1998]. We are continuing to work on resolving this discrepancy.

[16] Briefly, the simulation considers primary particles (protons and alpha particles) sampled randomly from a solar maximum spectrum appropriate for the northbound voyage. These particles are then propagated through the atmosphere using FLUKA and HEAVY particle transport packages [*Fassò et al.*, 1993; *Engel et al.*, 1992]. Sea-level particles are collected and are used as input to another simulation which propagates particles through a typical NM-64 structure using FLUKA and specialized software developed by one of the authors [*Clem*, 1999; *Clem and Dorman*, 2000]. The elapsed time between the starting position of the primary particle at the top of the atmosphere and thermal neutron detection is accumulated accordingly throughout the full calculation and is recorded along with other relevant parameters for primary and secondary particles. Further details of this simulation can be found in the work of *Clem and Dorman* [2000, and references therein].

[17] The right panel in Figure 1 displays the extended distribution of the same data shown in the left panel. This figure clearly reveals a break in the pure exponential distribution near 4 ms. Single cosmic ray events are randomly distributed in time, hence the resulting δT data should follow an exponential distribution of a fixed time constant. The break in the distribution separates single uncorrelated events from multiplicity events. These measurements show that most multiplicity events have δT values of less than 4 ms.

4. Results

[18] In Figure 2 we use our simulation to illustrate how the δT distribution contains information on the energy spectrum of the primary cosmic rays. For a series of intervals in δT, we show the median energy of the primary cosmic rays that produced counts having that value of δT. Points are plotted at the midpoint of each δT range. Fluctuations are mainly statistical due to the limited number of events generated in the simulation. The flat region (δT > 2 ms) in Figure 2 represents a pure random selection of primary cosmic rays

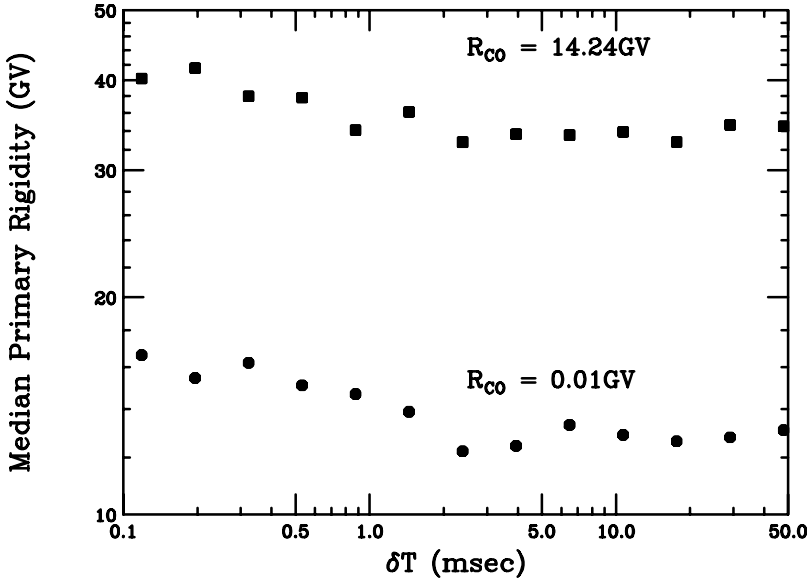

Figure 2. The median rigidity of the primary cosmic rays that produce counts with different values of δT.

with no biasing in rigidity. This region corresponds to the pure exponential section of the δT distribution in Figure 1 where primary cosmic rays produce a single count. At lower values in Figure 2 the upturn (δT < 2 ms) represents a transition from a random selection to a biased selection of primary cosmic rays with higher rigidities.

[19] In theory therefore recording multiplicity permits the sampling of different rigidity regions of the primary spectrum at a fixed location. Each bin in the δT distribution responds in a different way to the primary cosmic ray spectrum. In order to extract the primary cosmic ray spectrum from the δT distribution, a separate yield function for each δT component must be developed and used in an iterative numerical deconvolution. *Dorman et al.* [1981] discuss such an approach. Actual calculation of each yield function for an adequate number of δT ranges remains a future project for us. At present, our main focus is on the small but systematic deviations of our simulation from the observations. The simulations reproduce the trends quite well, but the normalization remains elusive in several respects. At this point it is not clear whether the problem lies in the method or is simply the result of small errors in cross sections propagating through the many generations of secondary particles that separate the primary cosmic rays from the recorded count rate of the monitor.

[20] One immediate application of our work is to assess the implications of the use of different choices for detector dead time on the performance of a neutron monitor. The original amplifier and discriminator circuits designed for the BP-28 counters have an average dead time of 20 μs to maximize the overall count rate while the early Russian/FSU stations introduced a 1200 μs dead time in an effort to move the response of the monitor to lower energy. It is very important to understand the implications of this choice

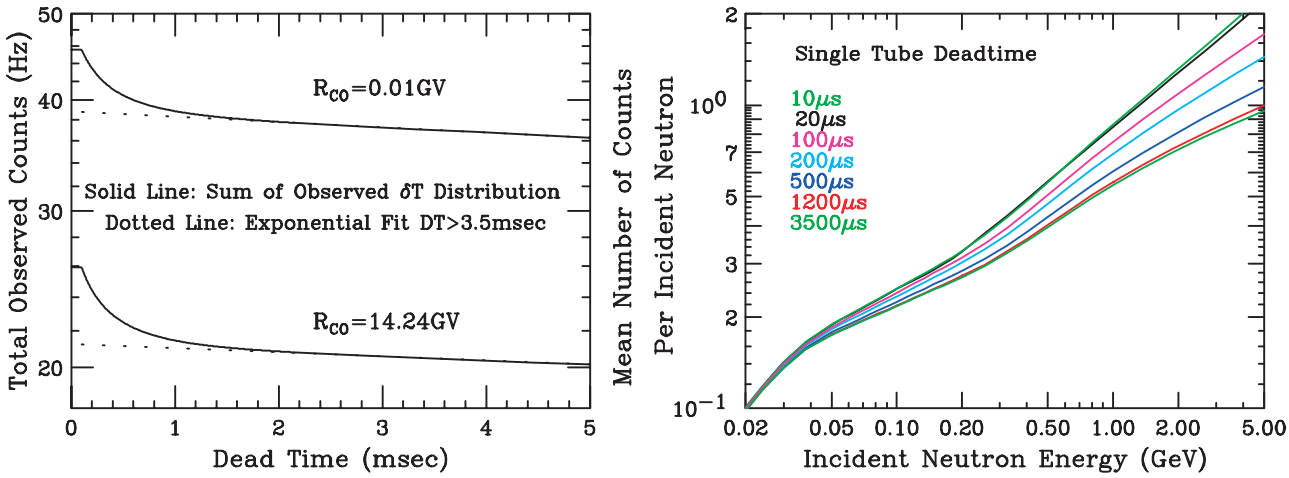

Figure 3. (left) The integral of δT distributions shown in Figure 1 as a function of the integral lower limit. The integral is the neutron monitor count rate when the dead time is the integral lower limit. (right) The average number of counts in a 6 tube NM-64 calculated for different dead times.

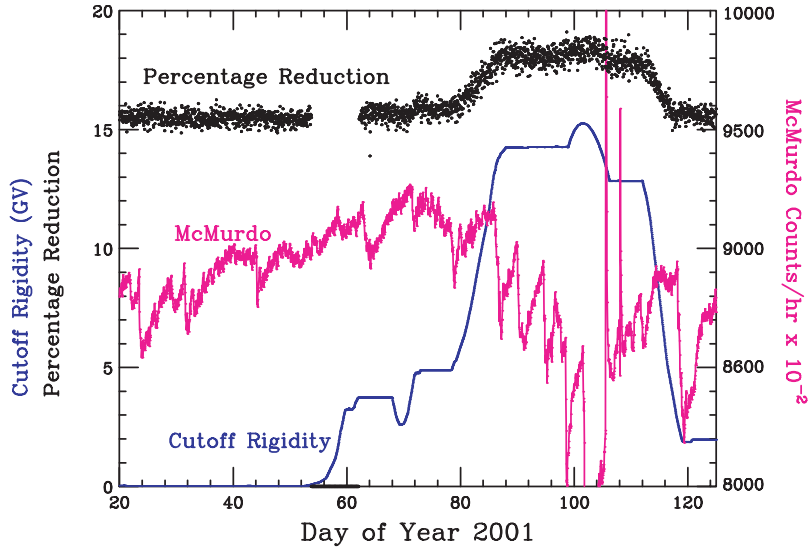

Figure 4. Time profile plot of the 2000–2001 latitude survey north bound voyage. The points show the percentage of counts having $\delta T < 1200$ μs. The McMurdo count rate provides an indicator of solar activity during the survey. The effective vertical cutoff rigidity is shown as a solid line. Flat regions of the solid line occur when the ship is moored. The data are hourly averages.

when reading the literature and using data from different stations in the same analysis. In the left panel of Figure 3 we show the result of summing the δT distributions from different lower limits. The actual distribution is compared in each case to an exponential (dotted line) fitted at high δT values. We use the simulation to generate the right panel of Figure 3, which shows the calculated average number of counts per incident neutron as a function of energy and dead time. These results show that the ability of an NM64 to detect multiple evaporation neutrons from a single incident particle is nearly maximized for a dead time of 20 μs and nearly minimized for 1200 μs. Unfortunately, the shorter dead time calculations can not be verified by our data since our multiplicity circuit has an intrinsic 95 μs dead time. According to our analysis these two dead times were well chosen to achieve the desired effect at the 1% level, however it would seem (refer back to Figure 1) that 4 ms dead time would be needed to achieve a pure nonmultiplicity event sample.

[21] Figure 3 clearly demonstrates the NM-64 response to primary cosmic rays is different for the dead time used for the early Russian/FSU stations and the standard NM-64 value. Since our multiplicity circuit has an intrinsic 95 μs dead time, we are unable to make a direct comparison between these two exact dead times, but a lower limit on the effect can be determined. Figure 4 displays the percentage

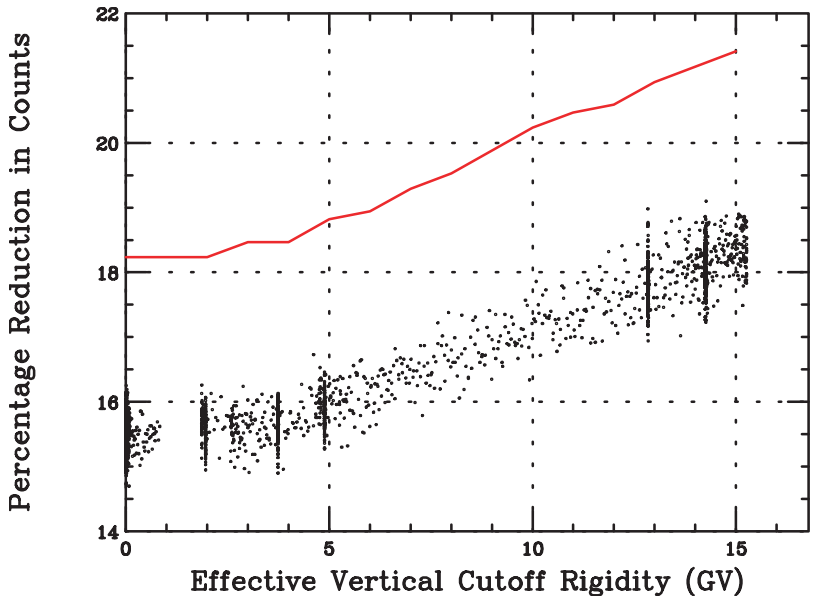

Figure 5. Observed percentage of counts having $\delta T < 1200$ μs as a function of effective vertical cutoff rigidity. The curve is the result of our simulation.

reduction in counts when the circuit dead time is changed from 95 μs to 1200 μs. This so called "Russian Reduction" is shown as a function of time during the 2000–2001 latitude survey along with the local effective vertical cutoff (GV) and McMurdo neutron monitor station count rates. The sun was very active during this period, but this activity had little effect on the "Russian Reduction" within observational error. These observations also imply that a Forbush decrease has very little effect on the ground spectral shape (recall from equation (2) the evaporation neutron multiplicity in the producer strongly depends on the incident energy), even though it reduces the overall flux level of sea level hadrons. However the "Russian Reduction" shows a fairly strong dependence on cutoff rigidity. In Figure 4 it increases with increasing rigidity which implies the early Russian/FSU stations were less sensitive to high-rigidity primaries. The cutoff rigidity thus has a significant effect on both the spectral shape and the overall flux level of sea level hadrons.

[22] Figure 5 displays as a direct correlation the percentage reduction and cutoff rigidity. The percentage reduction varies from 15.5% to 18.5% over a cutoff range from 0 to 15 GV. This dependence is quite significant, particularly since some research projects require neutron monitor accuracies better than a few percent. The rigidity dependence of the "Russian Reduction" would actually be stronger if the standard dead time of 20 μs were compared. The simulation result is also shown in this plot for comparison. The shape represents the observations fairly well, however the simulation is roughly 15% higher than the data. This difference derives from the minor difference in the shape of the calculation and observations shown in Figure 1. These anomalies in the calculation provide interesting clues for our ongoing investigation to understand the internal processes in a neutron monitor.

5. Summary

[23] Recording the full time structure of the neutron detections provides a powerful tool to study various characteristics of a neutron monitor. It allows us to better understand the statistics of count rates with and without multiplicity events. We have found that dead times greater than 1.2 ms reduce the contribution of multiplicity events to a level less than 1% and therefore simplify the count rate statistical nature to a pure Poisson distribution. Moreover the count rate with a dead time greater than 1.2 ms is more sensitive to changes in the lower energy regime of the primary cosmic ray spectrum than counts with a standard 20 μs dead time. From these observations it is obvious that the neutron monitor yield function depends on dead time and tends to have less variation with rigidity for larger dead times. Discrepancies remain between measurements and calculations, but the agreement (particularly with respect to trends in the data) is sufficiently good to permit interpolation of measured data and even limited extrapolation.

[24] **Acknowledgments.** We thank the officers and crew of the U.S. Coast guard cutter Polar Sea, Barry Wilson and Keith Bolton of the University of Tasmania, and the Bartol technical staff including Vanja Bucic, Len Shulman, and James Roth. This work was supported by NSF grant ATM-0000315.

[25] Shadia Rifai Habbal thanks Lev I. Dorman and another referee for their assistance in evaluating this paper.

References

Aleksanyan, T. M., V. M. Bednazhevsky, Y. L. Blokh, L. I. Dorman, and F. A. Starkov (1979), Coupling coefficients of the neutron component for the stars of various multiplicities inferred from the measurements on board research vessel Academician Kurchatov, *Proc. Int. Conf. Cosmic Rays 16th*, *4*, 315.

Bieber, J., J. Clem, M. L. Duldig, P. Evenson, J. E. Humble, and R. Pyle (2003), Cosmic ray spectra and the solar magnetic polarity: Preliminary results from 1994–2002, *Solar Wind Ten*, edited by M. Velli et al., *AIP Conf. Proc.*, *679*, 628.

Birattari, C., et al. (1998), The extended range neutron rem counter LINUS: Overview and latest developments, *Radiat. Prot. Dosimetry*, *76*, 135.

Blokh, Y. L., L. I. Dorman, N. S. Kaminer, and I. N. Kapustin (1971), Cosmic ray neutron spectrograph on the basis of registration channels with different dead times, *Geomagn. Aeron.*, *11*, 891.

Clem, J. M. (1999), Atmospheric yield functions and the response to secondary particles of neutron monitors, *Proc. Int. Conf. Cosmic Rays 26th*, *7*, 317.

Clem, J., and L. Dorman (2000), Neutron monitor response functions, *Space Sci. Rev.*, *93*, 335.

Clem, J. M., J. W. Bieber, P. Evenson, D. Hall, J. E. Humble, and M. Duldig (1997), Contribution of obliquely incident particles to neutron monitor counting rate, *J. Geophys. Res.*, *102*, 26,919.

Dorman, L. I., V. G. Yanke, and V. K. Korotkov (1981), Energy sensitivity of supermonitors to the multiple neutrons and the coupling functions, *Proc. Int. Conf. Cosmic Rays 17th*, *4*, 330.

Dorman, L. I., G. Villoresi, N. Iucci, M. Parisi, M. I. Tyasto, O. A. Danilova, and N. G. Ptitsyna (2000), Cosmic ray survey to Antarctica and coupling functions for neutron component near solar minimum (1996–1997): 3. Geomagnetic effects and coupling functions, *J. Geophys. Res.*, *105*, 21,047.

Dyring, E., and B. Sporre (1966), Latitude effect of neutron multiplicity as detected by a shipborne neutron monitor, *Ark. Geofys.*, *5*, 67.

Engel, J., T. Gaisser, P. Lipari, and T. Stanev (1992), Nucleus-nucleus collisions and interpretation of cosmic ray cascades, *Phys. Rev.*, *D46*, 5013.

Fassò, A., A. Ferrari, A. Ranft, P. R. Sala, G. R. Stevenson, and J. M. Zazula (1993), A comparison of FLUKA simulations with measurements of fluence and dose in calorimeter structures, *Nucl. Instrum. Methods*, *A332*, 459.

Hatton, C. (1971), The neutron monitor, *Progr. Elem. Part. Cosmic Ray Phys.*, *10*, 1.

Hatton, C., and E. Tomlinson (1968), The lifetime of neutrons in cosmic-ray neutron monitors, *Nuovo Cimento B*, *53*, 63.

Hughes, E., P. L. Marsden, G. Brooke, M. A. Meyer, and A. W. Wolfendale (1964), Neutron production by cosmic ray protons in lead, *Proc. Phys. Soc. London, Sect. A*, *83*, 239.

Iucci, N., G. Villoresi, L. I. Dorman, and M. Parisi (2000), Cosmic ray survey to Antarctica and coupling functions for neutron component near solar minimum (1996–1997): 2. Determination of meteorological effects, *J. Geophys. Res.*, *105*, 21,035.

Moraal, H., M. S. Potgieter, P. H. Stoker, and A. J. van der Walt (1989), Neutron monitor latitude survey of cosmic ray intensity during the 1986/1987 solar minimum, *J. Geophys. Res.*, *94*, 1459.

Nagashima, K., S. Sakakibara, and K. Murakami (1989), Response and yield functions of neutron monitor, galactic cosmic ray spectrum and its solar modulation, derived from all the available world-wide surveys, *Nuovo Cimento Soc. Ital. Fis. C*, *12*, 173.

Particle Data Group (2002), Review of particle physics, *Phys. Rev. D*, *66*, 84.

Shen, M. (1968), Neutron production in lead and energy response of neutron monitor, *Nuovo Cimento*, *VI*, suppl., 1177.

Shibata, S., et al. (1999), Calibration of neutron monitor using accelerator neutron beam, *Proc. Int. Conf. Cosmic Rays 26th*, *7*, 313.

Villoresi, G., L. I. Dorman, N. Iucci, and N. G. Ptitsyna (2000), Cosmic ray survey to Antarctica and coupling functions for neutron component near solar minimum (1996–1997): 1. Methodology and data quality assurance, *J. Geophys. Res.*, *105*, 21,025–21,034.

J. W. Bieber, J. M. Clem, P. A. Evenson, and R. Pyle, Bartol Research Institute, University of Delaware, 217 Sharp Lab, Newark, DE 19716, USA. (clem@bartol.udel.edu)

M. L. Duldig, Australian Antarctic Division, Kingston, Tasmania 7050, Australia.

J. E. Humble, School of Mathematics and Physics, University of Tasmania, Private Bag 21, Hobart, Tasmania 7001, Australia.